Atmospheric Pressure Non-thermal Plasma for Air Purification: Ions and Ionic Reactions Induced by dc+ Corona Discharges in Air Contaminated with Acetone and Methanol

Atmospheric pressure non-thermal plasma for air purification: ions and ionic reactions induced by dc+ corona discharges in air contaminated with acetone and methanol

Agata Giardina, Milko Schiorlin[#], Ester Marotta* and Cristina Paradisi

Department of Chemical Sciences, Università di Padova, via Marzolo 1, 35131 Padova, Italy

[#]*Present address:* Leibniz Institute for Plasma Science and Technology (INP Greifswald), F.-Hausdorff-Str. 2, D-17489 Greifswald, Germany

E-mail: ester.marotta@unipd.it

Abstract

Atmospheric pressure mass spectrometry (APCI-MS) was used to investigate the positive ions in air containing acetone (A), methanol (M) and mixtures thereof (A + M), subjected to +dc corona discharges. The results of experiments with isotopically labelled analogues, perdeuterated acetone A_{deu} and methanol M_{deu}, and relevant thermochemical data found in the literature allowed us to identify the main ionic reactions occurring in single component systems (A or M) and in binary mixtures (A + M). It is concluded that, thanks to its significantly higher proton affinity, A is very efficient in quenching M-derived ions at atmospheric pressure. These conclusions provide a rationale for interpreting the results of a parallel investigation on the reciprocal effects of M and A when treated together in air at atmospheric pressure with +dc corona in a non-thermal plasma reactor developed previously in our laboratory. Specifically, we observed a marked drop in the degradation efficiency of methanol when it was treated in the presence of an equivalent amount of acetone. This effect is attributed to acetone interfering with ion-initiated degradation processes of methanol, and supports that ions and ionic reactions are important in dc+ corona induced oxidation of volatile organic pollutants in air.

Keywords: corona discharges, VOC, advanced oxidation, ions in air plasma, atmospheric pressure mass spectrometry, air pollution control

Introduction

Corona discharges and dielectric barrier discharges in a gas at room temperature and atmospheric pressure generate non-thermal plasmas (NTP) which are useful in air purification treatments [1-3]. Laboratory-scale NTP set ups described in the literature for the removal of volatile organic compounds (VOCs) are based on different electrode configurations, energization modes, and reactor designs [2, 4]. Coupling of non-thermal plasma with heterogeneous catalysts and photocatalysts is also being applied with success in pursuit of synergic effects [5-8]. The achievements and knowledge gained over a few decades of fundamental research and modeling studies have led to the development of large scale pilot plants which are in operation in various parts of the world and to the commercialization of smaller devices for domestic use [1, 9]. Despite this rather advanced level of maturity of plasma based air purification technology there are still important aspects which need to be investigated in detail in fundamental research. These include among others the characterization of chemical reactions, products and mechanisms and of possible mutual interferences arising in treatment of air containing mixtures of various VOCs. This paper addresses both issues, as it reports and discusses the reciprocal effects of two model VOCs, acetone and methanol, when treated together in air at room temperature and atmospheric pressure with dc+ corona discharge and it also provides insight into the role of ionic intermediates and reactions in the degradation processes. Corona discharges are indeed a very convenient means to produce ions at atmospheric pressure and are widely used for this purpose in applications ranging from electrostatic precipitators to commercial instrumentation for mass spectrometric analyses. While the role of ions and ion-molecule reactions in non-thermal plasma based air purification treatments has been recognized and highlighted in several studies [10-18], the majority of mechanistic investigations on NTP induced degradation of

VOCs neglects their reactions with ions. Ions have been indeed classified as “less important plasma particles”, in contrast with neutral reactive species (atoms, radicals and excited molecules), in reason of their very fast reactions, orders of magnitude faster than radical-molecule reactions, and of the typically dilute concentrations of VOCs [8].

Previous work in our laboratories has investigated the ions in non thermal plasmas generated by corona discharges in VOC-contaminated air at atmospheric pressure. An Atmospheric Pressure Chemical Ionization – Mass Spectrometer (APCI-MS) was used to investigate the behavior of VOCs belonging to various classes of organic compounds, notably aliphatic [15, 19] and aromatic hydrocarbons [20], chlorinated hydrocarbons [14], halons and other fluoro-, perfluoro- and bromo-substituted alkanes [17, 21-23], and esters [18, 24]. In all cases, VOC-derived positive ions were the major species recorded at the mass spectrometer detector, in spite of the fact that the VOCs were present in low relative concentrations (typically a few tens to a few hundred ppm). This outcome is due, as detailed further in the paper, to the very fast redistribution of charge at atmospheric pressure via exothermic ion molecule reactions, notably proton transfer and electron transfer reactions from “background” ions to VOC molecules.

The present paper deals with mixtures of two important VOCs, acetone and methanol, chosen as representative models in reason of their wide diffusion in the environment and their occurrence as indoor organic pollutants in civil and industrial settings including wood processing and pulp mills plants [25]. Acetone is one of the most abundant oxygenated VOCs in air. It is both a primary pollutant, released as such in the atmosphere from its use as solvent in many products and applications, and a secondary pollutant, formed as a reaction intermediate in the tropospheric oxidation of hydrocarbons. It is relatively persistent in the troposphere, with an estimated lifetime due to reaction with OH radicals of 65 days [26]. Methanol is more reactive, its lifetime being 15 days [26]. Both methanol [27, 28 and refs. cited therein] and acetone [13, 29, 30] have been subjected to NTP based treatments in previous investigations employing different types of discharges and

reactors, processed alone and also together [25, 31] as well as in mixtures with other VOCs [32, 33]. In most cases, the mechanism proposed involves initial attack by reactive neutrals (OH radical, O atom) or homolytic dissociation following quenching of nitrogen metastable states. On the other hand, more than twenty years ago Penetrante et al. [27] proposed that reaction with positive ions is the most important initiation route for methanol degradation in air and nitrogen NTP generated by pulsed corona discharges. These and related data were used to develop a mathematical model by Derakhshesh et al. [34]. We provide in this paper experimental evidence for the involvement of VOC-derived ions and their reactions in NTP plasma produced by dc+ corona in air containing acetone, methanol and mixtures thereof.

Experimental

Chemicals. 'Air' used in the experiments was a syntethic mixture (80% nitrogen – 20% oxygen) from Air Liquide with specified impurities of H_2O (< 3 ppm) and of C_nH_m (< 0.5 ppm) ('synthetic air'). Acetone (>99.5% purity, HiPerSolv CHROMANORM), acetone-d_6 (99.9 atom % D, Sigma Aldrich), methanol (>99.5% purity, HiPerSolv CHROMANORM) and methanol-d_4 (99.8 atom % D, Sigma Aldrich) were used as received.

Corona reactor, gas line and experimental procedures. The corona reactor is described in detail in previous publications [17, 18, 20, 35]. It consists of a cylinder in stainless steel (38.5 mm i.d. x 600 mm) which is electrically grounded and has a small window (10 x 1 cm) cut through its wall for visual inspection of the plasma. The active electrode is a stainless steel wire (1 mm o.d.) fixed along the cylinder axis. The assembly is snugly enclosed into a pyrex cylinder of only slightly wider diameter and made leak-free by means of Teflon caps at both ends. The reactor can be energized by dc or pulsed high-voltage power. For this study a dc power supply with the following operating ranges was used: input voltage 0 – 220 V, output voltage -25 – +25 kV, output current 0 – 5 mA. To measure power input we used a digital oscilloscope (Tektronix 410A, bandwidth 200 MHz, two channels),

two high voltage probes (Beckman HV-211-22, ratio 1000:1, peak voltage 50 kVdc and Tektronix P6015, ratio 1000:1, bandwidth 75 MHz, peak voltage 40 kV), and two homemade current probes with 10 resistors in parallel housed in an electromagnetic shield (1.1 Ω for pulsed current and 52 Ω for dc current).

The reactor works in a flow-through mode of operation. It is connected to a gas line made of teflon tubing (4 mm i.d.) which allows to prepare and feed to the reactor the gas of desired composition, i.e. air contaminated with one or two VOCs each present at the set concentration (Figure 1). For this purpose, a flow of air is split into two portions, each going to a separate loop used to prepare the desired mixture of a single VOC in air (one loop for VOC 1 and one for VOC 2). Each loop is equipped with two flowmeters, a bubbler containing a sample of the liquid VOC and a mixing chamber (a 150 mL stainless steel canister lined with teflon). Proper adjustment of the two flows and of the liquid VOC volume and temperature in each loop allows to achieve the VOC desired concentration. Finally, the two flows containing the two different VOCs are mixed in a third mixing chamber and fed to the reactor. The VOCs initial concentration was determined by GC analysis and verified to remain stable in time prior to switching on the discharge. All experiments reported in this work were run at a constant gas flow rate of 500 $mL \cdot min^{-1}$ while changing the applied voltage and thus the SIE, the Specific Input Energy (kJ/L), which was determined as described previously [35]. The efficiency of the process was determined by measuring the VOCs residual concentration in the treated gas sampled at the reactor outlet as a function of SIE. The analyses were performed using a GC/TCD/FID (Agilent Technologies 7890). The experimental concentration data, [VOC], measured at given SIE values were interpolated with the exponential equation $[VOC]/[VOC]_0 = e^{-k_E \cdot SIE}$, where $[VOC]_0$ is the VOC initial concentration, to obtain the fitting constant, k_E, which is a measure of the process efficiency. Each experiment was carried out at least twice, the repeatability of the results being within 10%. After each experiment the reactor was “cleaned” by flowing pure air for several minutes prior to switching to the air/VOC mixture to be used in the next experiment.

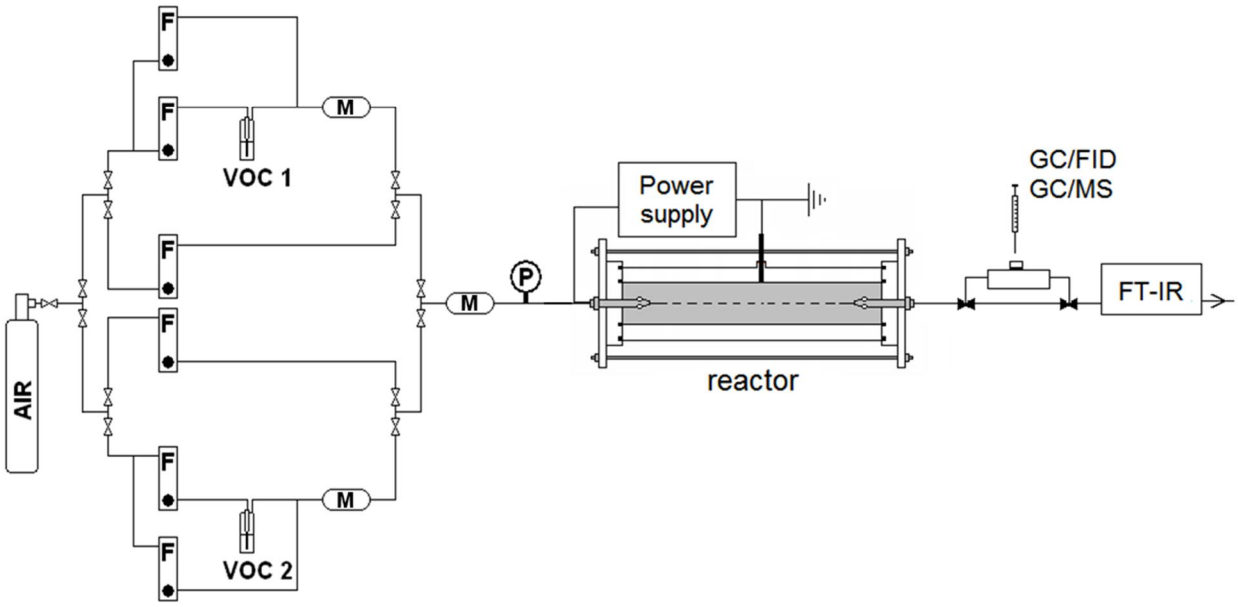

Figure 1. Schematics of corona discharge reactor and set-up used in this work for treatment of one VOC and binary VOC mixtures. **F**: flowmeter; **M**: mixing chamber; **P**: manometer.

Analysis of ions. Ion analysis was performed with an Atmospheric Pressure Chemical Ionization - mass spectrometer (APCI-TRIO 1000 II by Fisons Instruments, Manchester, U.K.) as described previously [14, 15, 19, 20, 36].

The APCI ion source operates at atmospheric pressure, with synthetic air flowing in at 4000-5000 $mL \cdot min^{-1}$ through the nebulizer. Vapors of the VOC of interest are stripped from a small liquid reservoir by an auxiliary flow of air (typically 5-50 $mL \cdot min^{-1}$) and enter the APCI source through a capillary (i.d. = 0.3 mm) running coaxially inside the nebulizer. Two such lines are available, one for each VOC, and allow to produce the mixture of desired composition. The VOC concentrations within the APCI source were determined by GC analysis of samples withdrawn at the source exhaust. Corona discharge occurs between a needle electrode set at + 3 kV and a counter electrode, held at 0-150 V relative to ground, shaped as a cone (the 'sampling cone') with an orifice of ca 50 μm in diameter on its tip. The ions leave the source through this orifice, cross a region pumped down to ca. 10^{-2} Torr and, through the orifice in a second conical electrode (the 'skimmer cone', kept at ground potential),

reach the low pressure region hosting the focusing lenses, the quadrupole analyzer and the detector. The ions kinetic energy and therefore their collision energy can be modulated by changing the voltage (V_{cone}) applied to the sampling cone. Analysis and comparison of spectra recorded at increasing values of V_{cone} (energy resolved spectra) provide information on the ions fragmentation behaviour and thus on their structure.

Results and Discussion

Efficiency of oxidation of methanol and acetone treated individually and together

Air contaminated with methanol (M), acetone (A) or methanol plus acetone was treated in our large non-thermal plasma flow-through reactor powered by +dc high voltage. Since our focus in this study was on the kinetics and mechanisms of VOC oxidation, reliable and reproducible results were mandatory, which can only be achieved under controlled and stable experimental conditions, including gas composition and flow and discharge and plasma stability. For this reason we did not use ambient air but a synthetic mixture of nitrogen and oxygen of high purity ("synthetic air", hereafter indicated simply as "air") and contaminated it with the desired concentration of one or both the VOCs considered. These mixtures were prepared by flowing synthetic air through a bubbler containing a liquid sample of the VOC of interest and by mixing this VOC containing air flow with one of pure air in proportions such as to reach the desired VOC concentration and total flow for the experiment (see schematics in Figure 1). For experiments with mixtures of the two VOCs, two such gas loops were used in parallel (Figure 1). The total gas flow through the reactor was always 500 mL/min which corresponds to a reaction time of 1.4 min. The VOC degradation profile as a function of supplied energy was obtained by performing a series of experiments in which the energy was changed by changing the applied voltage and the VOC residual concentration was measured by GC/FID at the reactor outlet. Approximately exponential decay profiles were typically obtained in these experiments, as exemplified by the plots in Figure 2. Values of k_E, the process energy constant,

obtained by interpolation of the experimental data with the first order exponential function are collected in Table 1, which includes the results of experiments in which A and M were treated individually at two different initial concentrations (250 and 500 ppm) and together, each at an initial concentration of 250 ppm.

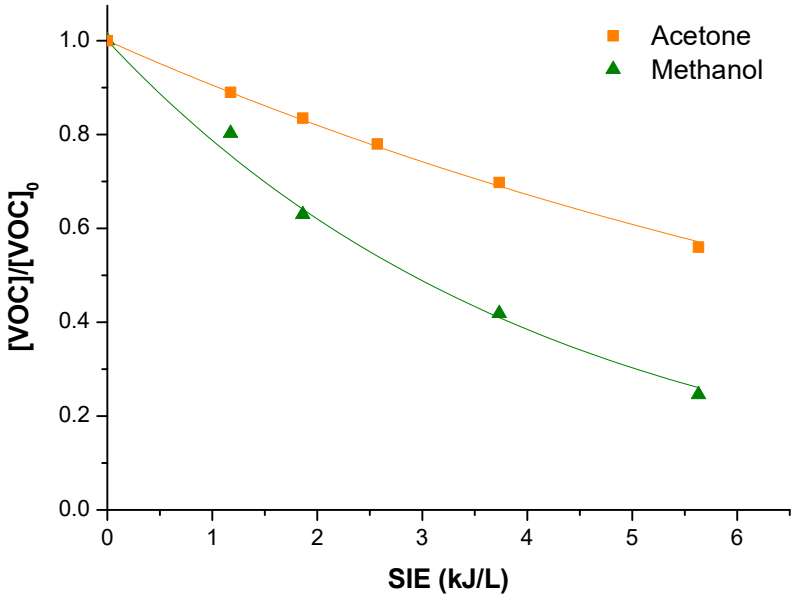

Figure 2. VOC conversion as a function SIE, the specific input energy, in dc+ corona treatment. Each VOC was treated individually at an initial concentration of 250 ppm in air at room temperature and atmospheric pressure.

Table 1. Efficiency of decomposition, expressed as k_E, of acetone (A) and methanol (M) treated individually and in mixture in pure air at room temperature and atmospheric pressure

Entry	$[A]_0$ (ppm_v)	$[M]_0$ (ppm_v)	k_E (A) ($L \cdot kJ^{-1}$)	k_E (M) ($L \cdot kJ^{-1}$)
1	-	500	-	0.49
2		250	-	0.58
3	500	-	0.090	-
4	250	-	0.14	-
5	250	250	0.10	0.24

The results of the experiments with a single VOC show that, both for A and M, the value of k_E increases as the VOC initial concentration is decreased. This inverse dependence of k_E on the VOC initial concentration has been observed in previous studies [13, 16-18, 37] and has been attributed to inhibition of the reaction of the primary VOC with plasma reactive species due to competition by its oxidation intermediates as originally proposed by Slater and Douglas-Hamilton [37]. A second observation concerns the different reactivity of the two investigated VOCs which clearly shows that under the same experimental conditions M is intrinsically more reactive than A (compare entries 1 and 3 for VOC initial concentration of 500 ppm, and entries 2 and 4 for VOC initial concentration of 250 ppm). Last and most interesting are the results obtained in experiments in which A and M were treated together (entry 5) each at an initial concentration of 250 ppm. These results are to be compared for each VOC with those obtained in the experiment in which each was treated individually at 500 ppm initial concentration. In other words we compare the results of the experiment in which A (250 ppm) competes with M (250 ppm) with those of the experiment in which A (250 ppm) competes with A (250 ppm). It is seen that the reaction efficiency of M is significantly reduced in the presence of an equivalent amount of A, k_E decreasing from 0.49 (entry 1) to 0.24 $L \cdot kJ^{-1}$ (entry 5). In contrast, there appears to be no significant effect due to the presence of M on the reaction efficiency of A, as can be appreciated by the k_E data reported in entries 3 (0.090 $L \cdot kJ^{-1}$) and 5 (0.10 $L \cdot kJ^{-1}$) which are equal within the experimental error in these determinations (10%).

One important fact to be considered in analyzing and interpreting the results of experiments with A + M mixtures is the possibility that M is produced as a byproduct of acetone degradation induced by electric discharges, as reported in a few papers [25, 31]. The formation of significant amounts of M from A could in principle provide a rationale for the lower efficiency of M degradation observed when treated in mixture with A than when treated alone. Using GC-MS analysis, we did not detect any methanol in the gas at the reactor outlet during treatment of acetone containing air. Our findings are consistent with those of other studies which failed to detect methanol among the byproducts of acetone oxidation [38]. They are also consistent with the intrinsic reactivity of methanol which in our

reactor is considerably higher than that of acetone. Specifically, the results obtained in experiment 5 cannot be explained considering that acetone degradation produces some methanol even under the absurd hypothesis that acetone is instantaneously and quantitatively converted into methanol producing an initial methanol concentration of 500 ppm because the k_E value determined for methanol in experiment 5 is lower than that in experiment 1. So there must be some specific phenomena causing the reduced reactivity of methanol in the presence of acetone.

Previous work has pointed out the important role played by ionized species and their reactions in dc+ corona induced oxidation of hydrocarbons and halogenated hydrocarbons in air [15-18, 20]. There are however no data, to the best of our knowledge, on the possible involvement of ionic decomposition pathways in the case of oxygen containing VOCs. Thus, in order to gain insight into the mechanisms of dc+ corona induced oxidation of M and A and on their reciprocal influence we carried out an investigation of their gas phase ion chemistry in air at atmospheric pressure.

Ions and ionic reactions induced by dc+ corona in air containing methanol, acetone and mixtures of methanol plus acetone

An APCI-MS instrument was used to investigate the ions generated by dc+ corona in air at atmospheric pressure and their reactions [36]. A typical spectrum recorded with pure synthetic air is shown in Fig. 3a.

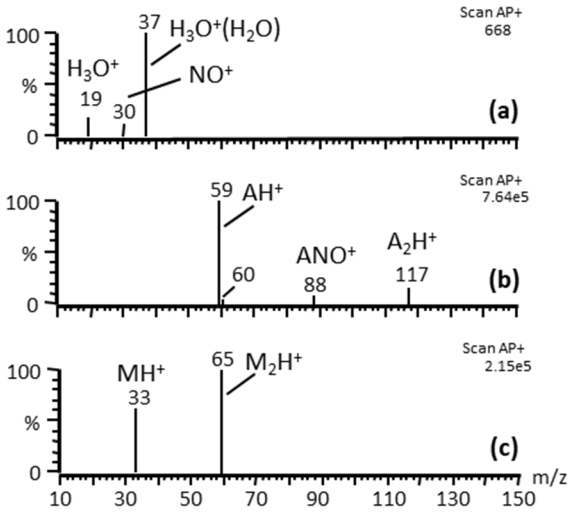

Figure 3. APCI positive mass spectra of a) pure air; b) acetone (500 ppm in air); c) methanol (500 ppm in air). All spectra were recorded at a voltage of 30 V applied to the counterelectrode, the sampling cone.

The observed signals are due to H_3O^+ (m/z 19), its hydrate $H_3O^+(H_2O)$ (m/z 37), and NO^+ (m/z 30). All are "secondary" ions formed via a cascade of fast exothermic reactions of the primary ions ($N_2^{+\bullet}$, $O_2^{+\bullet}$) produced by the interaction of high energy electrons with the main gas components, molecular nitrogen and oxygen. Remarkably, the hydronium ion and its clusters $H_3O^+(H_2O)_n$ are observed also when dry air is used, as was the case in this work, with a specified H_2O content of less than 3 ppm. This is the consequence of the fact that at atmospheric pressure exothermic reactions are very fast and thermodynamic equilibrium is reached within the ions residence time in the source (500 μs) [36], so the most stable ions are prevalent also if their precursors are present in very low concentration. The formation of hydronium ions and their hydrated clusters is accounted for by reactions (1) - (4).

1) $N_2^{+\bullet} + O_2 \rightarrow N_2 + O_2^{+\bullet}$

2) $O_2^{+\bullet} + H_2O + N_2 \rightarrow O_2(H_2O)^{+\bullet} + N_2$

3) $O_2(H_2O)^{+\bullet} + H_2O \rightarrow H_3O^+ + O_2 + {}^{\bullet}OH$

4) $H_3O^+(H_2O)_{n-1} + H_2O + N_2 \rightarrow H_3O^+(H_2O)_n + N_2$ n = 1, 2, 3, …

The size and relative amounts of cluster ions $H_3O^+(H_2O)_n$ depend not only on residual humidity and temperature but also on the ions kinetic energy, which is determined by the potential, V_{cone}, applied to the counterelectrode, the sampling cone. Thus, V_{cone} determines the energy of ion-neutral inelastic collisions and consequent collision induced ion dissociation and ultimately the appearance of the recorded spectrum. The spectrum reported in Fig. 3a was recorded with V_{cone} set at 30 V. By changing V_{cone} in the same experiment the recorded spectra changed drastically, as described in previous publications [22-24, 36]. Notably, at lower values of V_{cone} larger $H_3O^+(H_2O)_n$ clusters are observed which undergo collision induced declustering as V_{cone} is progressively increased.

As for NO^+, it can form from NO via charge exchange (eq. 5) or via ionic pathways (eq.s 6 -9).

5) $O_2^{+\bullet} + NO^\bullet \rightarrow NO^+ + O_2$

6) $N_2 + e^- \rightarrow N^+ + N^\bullet + 2e^-$

7) $N^+ + O_2 \rightarrow NO^+ + O$

8) $O_2 + e^- \rightarrow O^{+\bullet} + O + 2e^-$

9) $O^{+\bullet} + N_2 \rightarrow NO^+ + N^\bullet$

The presence of small amounts (500 ppm) of acetone or methanol in the air alters completely the mass spectra, as can be appreciated by comparison of the spectra reported in Fig. 3b - c with the "background" spectrum shown in Fig. 3a recorded with only air in the ion source. The signals of the "background" disappear and are substituted by VOC derived signals. Specifically, in the presence of acetone (A) the observed signals are due to AH^+ (m/z 59), ANO^+ (m/z 88) and A_2H^+ (m/z 117) (Fig. 3b), and with methanol (M), they are due MH^+ (m/z 33) and M_2H^+ (m/z 65) (Fig. 3c). Due to their low concentration (500 ppm), ionization of VOCs by interaction with high energy electrons is unlikely at atmospheric pressure, but rather occurs via ion-molecule reactions, notably proton transfer (10) and charge transfer reactions (11):

10) $VOC + H_3O^+ \rightarrow VOC{\cdot}H^+ + H_2O$ $\quad \Delta H = PA\ (X) - PA\ (VOC)$

11) $VOC + X^{+\bullet} \rightarrow VOC^{+\bullet} + X$ $\quad \Delta H = IE\ (VOC) - IE\ (X)$

where $X^{+\bullet} = O_2^{+\bullet}, N_2^{+\bullet}, H_2O^{+\bullet}$

Exothermic proton and electron transfer reactions generally occur at collision rate in the gas phase at atmospheric pressure. Thus, considering the thermochemical data reported in Table 2, reaction 10) is estimated to be very fast both for acetone and methanol, the reaction free enthalpy being – 121 and – 63.3 kJ·mol^{-1}, respectively. The same applies to ionization of acetone and methanol via charge transfer (reaction 11) to $N_2^{+\bullet}$, $O_2^{+\bullet}$ and $H_2O^{+\bullet}$. In contrast, since the ionization energy of NO is lower than that of either acetone or methanol, reaction 11) does not occur with NO^+.

Table 2. Ionization energy (IE) and proton affinity (PA) data (in kJ·mol^{-1}).[a)]

	N_2	**O_2**	**H_2O**	**NO**	**Acetone**	**Methanol**
PA	493.8	421	691.0	531.8	812.0	754.3
IE	15.581 ± 0.008	12.0697 ± 0.0002	12.621 ± 0.002	9.2642 ± 0.00002	9.703 ± 0.006	10.84 ± 0.01

a) Ref. [39]

It was shown previously [14, 15, 17-24] that the study of energy resolved mass spectra is most useful to characterize the ions structure and reactions. As described above, in these experiments the ions kinetic energy is changed by changing V_{cone}, the voltage applied to the counter electrode, the sampling cone. Depending on their kinetic energy, the ions inelastic collisions with molecules of the background gas will be more or less energetic and lead to ion declustering and fragmentation reactions. The results of such an investigation applied to acetone (500 ppm in air) are summarized in Fig. 4a which collects the data obtained in spectra recorded at different values of V_{cone} and shows the major ions relative intensities as a function of the ions kinetic energy. To aid interpreting the data of Fig. 4 and the following figures the major ions observed in these experiments and corresponding m/z values are collected in Table 3.

Table 3. Major stable ions detected in air containing acetone (A), methanol (M) and their perdeuterated analogues, A_{deu} and M_{deu}.

Acetone

A				A_{deu}					
AH^+	A_2H^+	ANO^+	A_2NO^+	$A_{deu}H^+$	$A_{deu}D^+$	$A_{deu2}H^+$	$A_{deu2}D^+$	$A_{deu}NO^+$	$A_{deu2}NO^+$
59	117	88	146	65	66	129	130	94	158

Methanol

M				M_{deu}					
MH^+	M_2H^+	M_3H^+	M_4H^+	$M_{deu}H^+$	$M_{deu}D^+$	$M_{deu2}H^+$	$M_{deu2}D^+$	$M_{deu3}H^+$	$M_{deu3}D^+$
33	65	97	129	37	38	73	74	109	110

Acetone + Methanol

A + M			A_{deu} + M	A + M_{deu}	
AMH^+	A_2MH^+	AM_2H^+	$A_{deu2}MH^+$	$A_2M_{deu}H^+$	$A_2M_{deu}D^+$
91	149	123	161	153	154

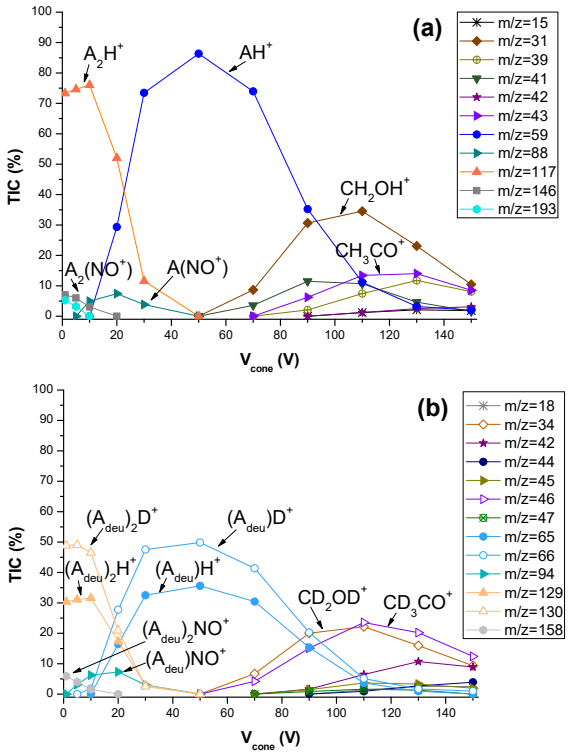

Figure 4. Relative intensities of positive ion signals as a function of energy in APCI-MS spectra of air containing: a) acetone, A, (500 ppm); b) perdeuterated acetone, A_{deu}, (500 ppm).

Acetone (A) ion chemistry is dominated by the protonated species AH^+ (m/z 59) which, at low kinetic energies, is detected as the ion-molecule cluster A_2H^+ (m/z 117). Weaker signals observed at low energies are due to $A(NO^+)$ (m/z 88), $A_2(NO^+)$ (m/z 146) and to the hydrate $A_2H^+(H_2O)$ (m/z 193). Increasing the ions kinetic energy induces declustering, as seen in Fig. 3a by the drop of the signal intensity of A_2H^+ and corresponding increase of that due to AH^+. At higher energies ion fragmentation occurs leading to product ions CH_3CO^+ (m/z 45), CH_2OH^+ (m/z 31) and CH_3^+ (m/z 15). In particular, the major observed product ion observed at V_{cone} values greater than 90 V is CH_2OH^+, a known fragmentation product of protonated acetone formed under collision-induced dissociation conditions [40].

Important insight into the origin and the reactions of protonated species was gained by performing experiments with perdeuterated acetone, CD_3COCD_3 (A_{deu}) (99.9% - deuterium enriched). The results, displayed in Figure 4b, show that major signals in the mass spectra are due to $A_{deu}D^+$ (m/z

66) and to its ion-molecule cluster $(A_{deu})_2D^+$ (m/z 130), accompanied by somewhat weaker signals due to protonated analogues $(A_{deu})H^+$ (m/z 65) and $(A_{deu})_2H^+$ (m/z 129). $A_{deu}(NO^+)$ (m/z 94) and $(A_{deu})_2$ (NO^+) (m/z 158) are also detected at low energies, whereas at higher energies (V ≥ 90 V) fragment ions CD_3CO^+, CD_2OD^+ and CD_3^+ are produced.

The formation of $A_{deu}D^+$ can be accounted for by reactions 12) and 13), whereas that of $A_{deu}H^+$ by reactions 14)-15). Based on available relevant thermochemical data, collected in Table 4, and neglecting possible differences due to the presence of D in place of H, most of these reactions are exothermic and therefore occur at the collision rate. Reaction 15) is endothermic but nevertheless is expected to occur due to the high energy of $A_{deu}^{+\bullet}$ formed in reaction 12).

12) $X^\bullet + CD_3COCD_3 \rightarrow M + CD_3COCD_3^{+\bullet}$ ΔH = -228, -567, -281.5 kJ·mol^{-1} for X = O_2, N_2, H_2O

13) $CD_3COCD_3^{+\bullet} + CD_3COCD_3 \rightarrow {}^\bullet CD_2COCD_3 + (CD_3COCD_3)D^+$ $\Delta H = -4.2$ kJ·mol^{-1}

14) $H_3O^+ + CD_3COCD_3 \rightarrow H_2O + (CD_3COCD_3)H^+$ $\Delta H = -121$ kJ·mol^{-1}

15) $CD_3COCD_3^{+\bullet} + H_2O \rightarrow {}^\bullet OH + (CD_3COCD_3)H^+$ $\Delta H = +51.6$ kJ·mol^{-1}

It should be noted that due to the high exothermicity of charge exchange reactions 12) fragmentation of ionized acetone can also occur, as shown in Scheme 1, leading to fragment ions CD_3CO^+ (the appearance energy of CH_3CO^+ is within 10.2-12.2 eV) [39] and CD_3^+ (the appearance energy of CH_3^+ is 15 eV) [39].

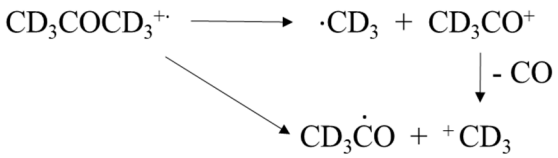

Scheme 1

In the plasma these fragment ions could react via proton transfer to acetone (eq.s 16 and 17).

16) $CD_3CO^+ + CD_3COCD_3 \rightarrow CD_2CO + (CD_3COCD_3)D^+$ $\Delta H = +7.8$ kJ·mol^{-1}

17) $CD_3^+ + CD_3COCD_3 \rightarrow CD_2 + (CD_3COCD_3)D^+$ $\Delta H = 0$ kJ·mol^{-1}

It should also be noted that reactive radicals form in some of these reactions, including carbon radicals ($^{\bullet}CD_2COCD_3$, $^{\bullet}CH_3$ and $CD_3C^{\bullet}O$) and $^{\bullet}OH$, which can contribute to radical-induced degradation of other VOC molecules.

Table 4. Free enthalpy of formation data (in $kJ \cdot mol^{-1}$) of relevant species.[a)]

Neutrals (molecules and radicals)

Species	H_2O	CH_3COCH_3	CH_3OH	CH_2CO	$:CH_2$	$\cdot OH$	$\cdot CH_2COCH_3$	$\cdot CH_2OH$
$\Delta H_f°$	-241.8	-218.5	-201.6	-47.7	+390	+39	-6.5	-25.9

Ions

Species	$[CH_3COCH_3]^{+}\cdot$	$[CH_3OH]^{+}\cdot$	$(CH_3COCH_3)H^+$	$(CH_3OH)H^+$	CH_3CO^+	CH_3^+
$\Delta H_f°$	+719.2	+845.3	+490	+567	+653	+1098

[a)] Ref. [39]

Similar investigations were also carried out with methanol (M) and perdeuterated methanol, CD_3OD, (M_{deu}). The results of these experiments are summarized in Figures 5a and 5b for M and M_{deu}, respectively. Similarly to what observed with acetone, the gas phase ion chemistry of methanol at atmospheric pressure is dominated by the protonated species MH^+ (m/z 33), which at low energies is detected as ion-molecule clusters M_4H^+ (m/z 129), M_3H^+ (m/z 97) and M_2H^+ (m/z 65) (Figure 5a). At higher energies (V > 50 V) the ionic fragment CH_3^+ is formed. With M_{deu} the corresponding fully deuterated ions are observed, $(M_{deu})D^+$ and its clusters $(M_{deu})_nD^+$ (n = 2, 3, 4), alongside with minor amounts of the corresponding protonated analogues $(M_{deu})_nH^+$ (Figure 5b).

Possible ionization routes are described in eq.s 18) – 21).

18) $X^{+\bullet} + CD_3OD \rightarrow X + CD_3OD^{+\bullet}$ $\Delta H = -457.4, -118.6, -171.8\ kJ \cdot mol^{-1}$ for $X = N_2$, O_2, H_2O

19) $CD_3OD^{+\bullet} + CD_3OD \rightarrow {}^{\bullet}CD_2OD + (CD_3OD)D^+$ $\Delta H = -102.6\ kJ \cdot mol^{-1}$

20) $H_3O^+ + CD_3OD \rightarrow H_2O + (CD_3OD)H^+$ $\Delta H = -63.3\ kJ{\cdot}mol^{-1}$

21) $CD_3OD^{+\bullet} + H_2O \rightarrow {}^{\bullet}OH + (CD_3OD)H^+$ $\Delta H = +2.5\ kJ{\cdot}mol^{-1}$

Reactions 18) -19) account for the formation of $(CD_3OD)D^+$ whereas reactions 20) - 21) account for the formation of $(CD_3OD)H^+$.

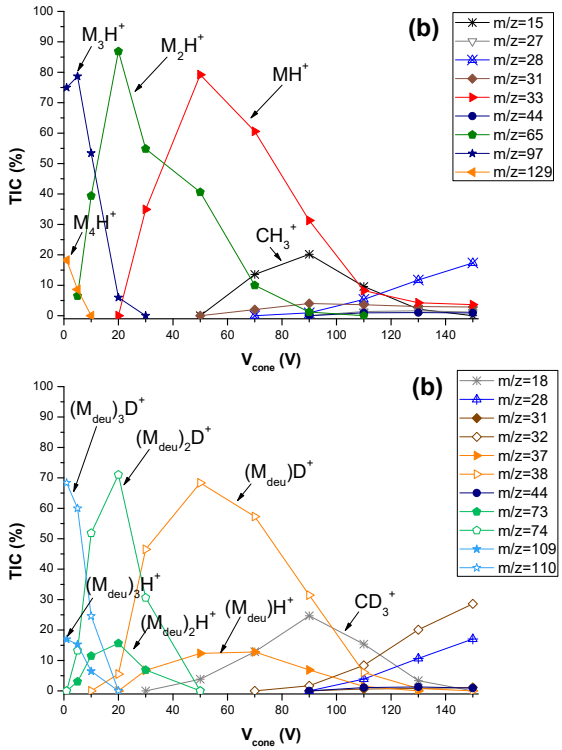

Figure 5. Relative intensities of positive ion signals as a function of energy in APCI-MS spectra of air containing: a) methanol, M, (500 ppm); b) perdeuterated methanol, M_{deu}, (500 ppm).

Experiments with acetone (A)/methanol (M) mixtures were carried out next using the following relative amounts: A/M = 1:1, 1:10 and 1:100. The results are displayed in Figure 6.

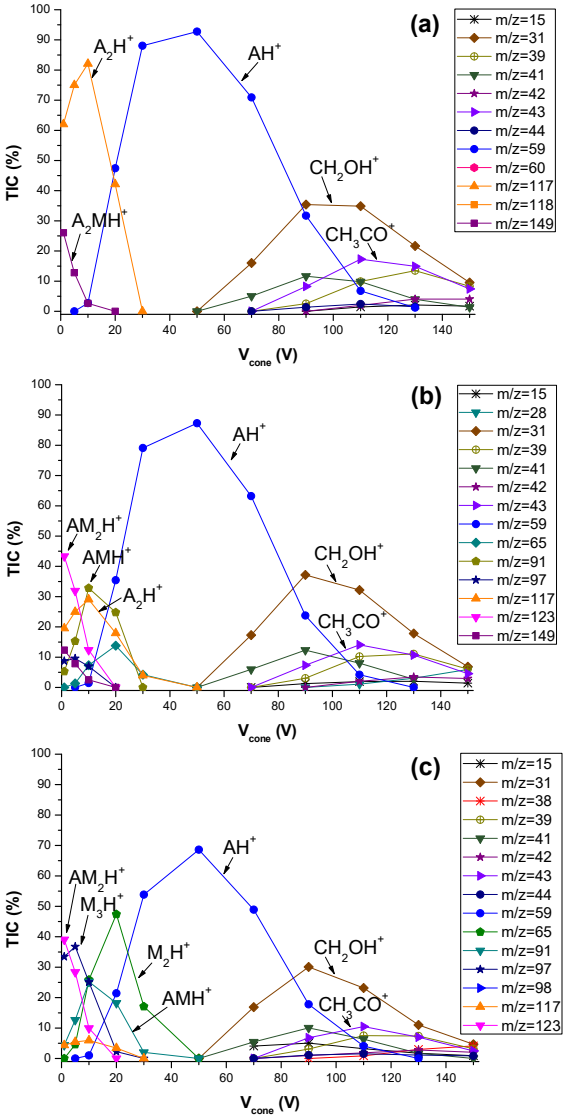

Figure 6. Relative intensities of positive ion signals as a function of energy in APCI-MS spectra of air containing mixtures of acetone (A) and methanol (M) in the following ratio: a) 1:1; b) 10:1; c) 100:1.

It is seen that the mass spectra of these binary mixtures are dominated by signals due to acetone derived ions, notably AH^+, A_2H^+ and their fragments, also in mixtures in which acetone is a minor component (Fig. 5c, A/M = 1:100). These observations are consistent with the higher proton affinity of acetone which makes proton transfer from MH^+ to A exothermic by 61.4 kJ·mol^{-1}. $M_nA_mH^+$ (m/z 91, 123, 149) and M_nH^+ (m/z 97, 65) can be observed at lower values of V_{smpl}, with n > 1only when methanol is at least in tenfold excess with respect to acetone (Fig.s 6b and c).

Isotope labelling was also applied to binary mixtures of acetone and methanol. Two kinds of mixtures were prepared and analyzed: perdeuterated acetone (A_{deu}) with methanol (M) and acetone (A) plus perdeuterated methanol (M_{deu}), each tested at two different compositions: A/M = 1:1 and 1:10. The results of these experiments are collected in Figure 7.

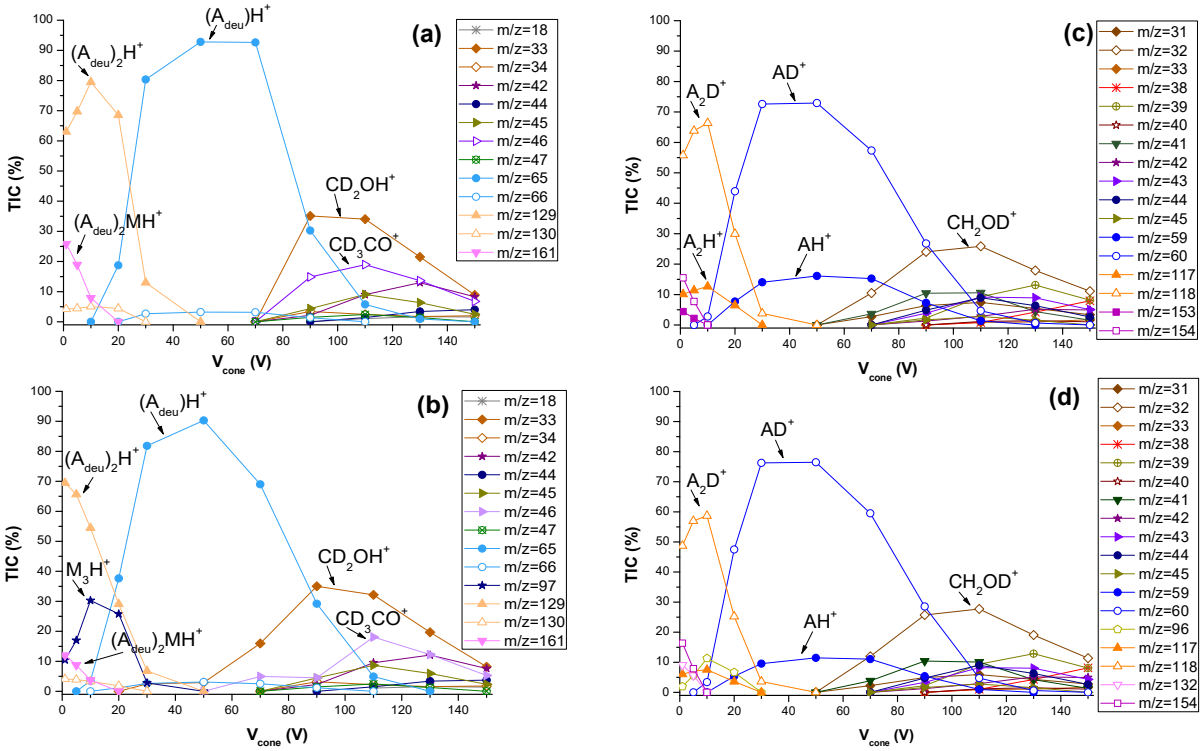

Figure 7. Relative intensities of positive ion signals as a function of energy in APCI-MS spectra of air containing mixtures of acetone and methanol in the following ratio: a) A_{deu}/M = 1:1; b) A_{deu}/M = 1:10; c) A/M_{deu} = 1:1; d) A/M_{deu} = 1:10.

The data confirm what observed with unlabeled A and M (Figure 6) as they show that even when methanol is in large excess with respect to acetone the mass spectra are dominated by the signals of protonated acetone and its ion-molecule complexes. In addition they provide clear indications that the reactions leading to the prevailing ions observed in methanol/acetone binary mixtures are the following:

22) $CX_3OX^{+\bullet} + CX_3OX \rightarrow {}^{\bullet}CX_2OX + (CX_3OX)X^+$ $\Delta H = -102.6$ kJ·mol^{-1}

23) $(CX_3OX)X^+ + CY_3COCY_3 \rightarrow CX_3OX + (CY_3COCY_3)Y^+ \quad \Delta H = -61.4\ kJ \cdot mol^{-1}$

X, Y = H, D

This scheme is consistent with the observation of $A_{deu}H^+$ (and complexes thereof) in A_{deu}/M mixtures (X = H, Y = D) and of $AM_{deu}D^+$ (and complexes thereof) in A/M_{deu} mixtures (X = D, Y = H). Notably, both reactions are strongly exothermic (the reported values of ΔH refer to X = H. They are not expected to differ significantly for X = D).

Conclusions

The results reported in the first part of this paper show that methanol is significantly more reactive than acetone in dc+ corona induced advanced oxidation in our non-thermal plasma reactor. However, when treated in mixture with an equivalent amount of acetone, the efficiency of methanol degradation was significantly reduced. Clues to rationalize the reciprocal effects observed when the two VOCs are treated together were gained by mass spectrometric analysis of the ions generated by corona discharge in air containing acetone and methanol and of their ion-molecule reactions. The results show indeed that, thanks to its considerably higher proton affinity, acetone quenches all methanol derived ions quite effectively also when methanol is present in 100-fold excess. It seems therefore reasonable to associate the drop in the degradation efficiency of methanol observed in the presence of acetone to the inhibition observed in our mass spectrometric investigation of all ionic reaction pathways contributing to methanol decay. The results obtained in this investigation also provide experimental evidence in support of the proposal that ionic reactions are major initiation steps in methanol degradation in NTPs produced by positive corona discharges [27].

Acknowledgments. The authors thank GioloCenter for financial support to their research on VOC decomposition by application of non-thermal plasma.

References

1. Kim HH (2004) Nonthermal plasma processing for air-pollution control: a historical review, current issues, and future prospects. Plasma Process Polym 1:91–110
2. Fridman A (2008) Plasma chemistry. Cambridge University Press, Cambridge.
3. Schiavon M, Torretta V, Casazza A, Ragazzi M (2017) Non-thermal plasma as an innovative option for the abatement of volatile organic compounds: a review. Water Air Soil Pollut 228:388
4. Xiao G, Xu W, Wu R, Ni M, Du C, Gao X, Luo Z, Cen K (2014) Non-thermal plasmas for VOCs abatement. Plasma Chem Plasma Process 34:1033–1065
5. Vandenbroucke AM, Morent R, De Geyter N, Leys C (2011) Non-thermal plasmas for non-catalytic and catalytic VOC abatement. J Hazard Mater 195:30–54
6. Zhang Z, Jiang Z and Shangguan W (2016) Low-temperature catalysis for VOCs removal in technology and application: A state-of-the-art review. Catal Today 26:270-278
7. Yao X, Jiang N, Li J, Lu N, Shang K, Wu Y (2019) An improved corona discharge ignited by oxide cathodes with high secondary electron emission for toluene degradation. Chem Eng J 362: 339-348
8. Kim HH, Teramoto Y, Ogata A (2019) Plasma-Catalyst Interactions. In: Tu X, Whitehead J, Nozaki T (eds) Plasma Catalysis. Springer Series on Atomic, Optical, and Plasma Physics, vol 106. Springer, Cham, Switzerland
9. Du C, Gong X, Lin Y (2019) Decomposition of volatile organic compounds using corona discharge plasma technology. J Air Waste Manag Assoc 69:879-899
10. Penetrante BM, Hsiao MC, Bardsley JN, Merritt BT, Vogtlin GE, Wallmann PH (1996) Electron beam and pulsed corona processing of volatile organic compounds in gas streams. Pure Appl Chem 68:1083-1087
11. Krasnoperov LN, Krishtopa LG, Bozzelli JW (1997) Study of volatile organic compounds destruction by dielectric barrier corona discharge. J Adv Oxid Technol 2:248-256

12. Sieck LW, Buckley TJ, Herron JT, Green DS (2001) Pulsed electron.beam ionization of humid air and humid air/toluene mixtures: time-resolved cationic kinetics and comparison with predictive models. Plasma Chem Plasma Process 21:441-457
13. Rudolph R, Francke KP, Miessner H (2002) Concentration dependence of VOC decomposition by dielectric barrier discharges. Plasma Chem Plasma Process 22:401-412
14. Marotta E, Scorrano G, Paradisi C (2005) Ionic reactions of chlorinated VOCs in air plasma at atmospheric pressure. Plasma Process Polym 2:209-217
15. Marotta E, Callea A, Ren X, Rea M, Paradisi C (2007) DC corona electric discharges for air pollution control. Part 2. Ionic intermediates and mechanisms of hydrocarbon processing. Plasma Process Polym 5:146-154
16. Marotta E, Schiorlin M, Rea M, Paradisi C (2010) Products and mechanisms of the oxidation of organic compounds in atmospheric air plasmas. J Phys D Appl Phys 43:124011
17. Schiorlin M, Marotta Dal Molin M, Paradisi C (2013) Oxidation mechanisms of CF_2Br_2 and CH_2Br_2 induced by air nonthermal plasma. Environ Sci Technol 47:542-548
18. Perillo R, Ferracin E, Giardina A, Marotta E, Paradisi C (2019) Efficiency, products and mechanisms of ethyl acetate oxidative degradation in air non-thermal plasma. J Phys D Appl Phys 52:295206
19. Marotta E, Paradisi C (2009) A mass spectrometry study of alkanes in air plasma at atmospheric pressure. J Am Mass Spectrom Soc 20:697-707
20. Schiorlin M, Marotta E, Rea M, Paradisi C (2009) Comparison of toluene removal in air at atmospheric conditions by different corona discharges. Environ Sci Technol 24:9386-9392
21. Marotta E, Paradisi C, Scorrano G (2004) An atmospheric pressure chemical ionization study of the positive and negative ion chemistry of the hydrofluorocarbons 1,1-difluoroethane (HFC-152a) and 1,1,1,2-tetrafluoroethane (HFC-134a) and of perfluoro-n-hexane (FC-72) in air plasma at atmospheric pressure. J Mass Spectrom 39:791-801

22. Marotta E, Bosa E, Scorrano G, Paradisi C (2005) Positive and negative ion chemistry of the anesthetic halothane (1-bromo-1-chloro-2,2,2-trifluoroethane) in air plasma at atmospheric pressure. Rapid Commun Mass Spectrom 19:391-396
23. Marotta E, Cooks RG, Paradisi C (2005) Novel CFCs-substitutes recommended by EPA (hydrofluorocarbon-245fa and hydrofluoroether 7100): ion chemistry in air plasma and reactions with atmospheric ions. E. Marotta, R. G., C. Paradisi. J Am Mass Spectrom Soc 16:1081-1092
24. Marotta E, Paradisi C (2005) Positive ion chemistry of esters of carboxylic acids in air plasma at atmospheric pressure. J Mass Spectrom 40:1583-1589
25. Sobacchi MG, Saveliev AV, Fridman AA, Gutsol AF, Kennedy LA (2003) Experimental assessment of pulsed corona discharge for treatment of VOCs emissions. Plasma Chem Plasma Process 23:347-370.
26. Hester RE, Harrison RM, Atkinson R (1995) Gas phase tropospheric chemistry of organic compounds. In: Volatile organic compounds in the atmosphere, Series: Issues in Environmental Science and Technology, Harrison RM, Hester RE (eds). The Royal Society of Chemistry
27. Penetrante BM, Hsiao MC, Bardsley JN, Merritt BT, Vogtlin GE, Kuthi A, Burkhart CP, Bayless JR (1997) Identification of mechanisms for decomposition of air pollutants by non-thermal plasma processing. Plasma Sources Sci Technol 6:251- 259
28. Norsic C, Tatibouët JM, Batiot-Dupeyrat C, Fourré E (2018) Methanol oxidation in dry and humid air by dielectric barrier discharge plasma combined with MnO_2-CuO based catalysts. Chem Eng J 347:944-952
29. Pasquiers S, Blin-Simiand N, Magne L (2016) Dissociation against oxidation kinetics for the conversion of VOCs in non-thermal plasmas of atmospheric gases. EPJ Appl Phys 75:150575
30. Rohani V, Affonso Nobrega P P, Zadeh M, Cauneau F, Fulcheri L (2017) Combination of VOC degradation and electro-hydrodynamic pumping actions in a surface dielectric barrier discharge reactor. Chem Eng J 309:471-479

31. Li X, Guo T, Peng Z, Xu L, Dong J, Cheng P, Zhou Z (2019) Real-time monitoring and quantification of organic by-products and mechanism study of acetone decomposition in a dielectric barrier discharge reactor. Environ Sci Pollut Res 26:6773–6781.
32. Chang CL, Lin TS (2005) Decomposition of toluene and acetone in packed dielectric barrier discharge reactors. Plasma Chem Plasma Process 25:227–243
33. Hou, L, Li X, Xie D, Wang H (2018) Effects of BTEX on the removal of acetone in a coaxial non-thermal plasma reactor: Role analysis of the methyl group. Molecules 23:890
34. Derakhshesh M, Abedi J, Hassanzadeh H (2010) Mechanism of methanol decomposition by non-thermal plasma. J Electrostat 68:424-428
35. Marotta E, Callea A, Rea M, Paradisi C (2007) DC corona electric discharges for air pollution control. Part 1. Efficiency and products of hydrocarbon processing. Environ Sci Technol 41:5862-5868
36. Donò A, Paradisi C, Scorrano G (1997) Abatement of volatile organic compounds by corona discharge. a study of the reactivity of trichloroethylene under atmospheric conditions. Rapid Commun Mass Spectrom 11:1687-1694
37. Slater C, Douglas-Hamilton DH (1981)Electron beam initiated destruction of low concentration of vinyl chloride in carrier gases. J Appl Phys 9:5820-5828
38. Zhao X, Liu X, Liu J, Chen J, Fu S, Zhong F (2019) The effect of ionization energy and hydrogen weight fraction on the non-thermal plasma volatile organic compounds removal efficiency. J Phys D Appl Phys 52:145201
39. Lias SG. Ionization energy evaluation. In NIST Chemistry WebBook, NIST Standard Reference Database No. 69, Maillard WG, Linstrom PJ (eds). National Institute of Standards and Technology: Gaithersburg MD, 2004. Available: http://webbook.nist.gov/chemistry/
40. Mair C, Fiegele T, Biasioli F, Herman Z, Märk TD (1999) Surface-induced reactions of acetone cluster ions. J Chem Phys 111:2770-2778 (Marotta 2007)